September 2011 / version 1.0

twoPionGen: a Monte Carlo event generator for $\pi^+\pi^-$ production in $\bar{p}p$ interactions

Manuel Zambrana[1], Dmitry Khaneft[2], Bertalan Feher, Eric Göbel, Yue Ma, Frank Maas, María del Carmen Mora, Cristina Morales, Roberto Pérez, David Rodríguez and Iris Zimmermann

Institut für Kernphysik, University of Mainz, Becher Weg 45, D-55128 Mainz
Helmholtz Institute Mainz, University of Mainz, D-55128 Mainz

Abstract

A Monte Carlo event generator for the process $\bar{p}p \to \pi^+\pi^-$, when both the proton target and the antiproton beam are unpolarized, is described. The kinematic region covers the antiproton momentum range from 0.79 GeV to 12.0 GeV, in the LAB frame. For the low energy regime, the parametrization of the cross section is based on a Legendre polynomial fit to data from the (antiproton beam) CERN 28 GeV proton synchroton. For the high energy regime, the recent predictions by J. van de Wiele and S. Ong based on a Regge Theory approach were used. The generator is a useful first tool to study pion production at PANDA.

[1]email: zambrana@kph.uni-mainz.de
[2]email: khaneftd@kph.uni-mainz.de

Contents

1 Introduction **1**

2 Kinematics **1**

3 The cross section **4**

4 Sampling the cross section **7**

5 Routines in the generator **7**

6 Interface to PandaRoot **8**

7 User guide **9**

8 Examples **9**

9 Summary **10**

A An example simulation macro **12**

1 Introduction

The availability of a high-intensity antiproton beam up to 15 GeV at the FAIR facility and of the PANDA detector offers unique possibilities for new investigations of the hadron structure (see [1] for a review). Feasibility studies for the determination of the proton electromagnetic form factors in the time-like region [2] with the PANDA detector have been already performed through the annihilation process $\bar{p}p \to l^+l^-$, with $l = e$ or μ, at several antiproton beam energies [3]. At the lowest order, the underlying mechanism is assumed to be the exchange of one virtual photon of four-momentum squared q^2, although the sensitivity of the measurement to higher exchanges was also investigated. The difficulty of the measurement is related to the hadronic background, mostly annihilation into pions, which is estimated to be about six orders of magnitude larger than the production of the lepton pair. The development of efficient algorithms for pion rejection requires the use of realistic Monte Carlo event generators for pion production, so the differences in the distributions of the relevant kinematic variables can be used to tune the cuts needed to discriminate the signal from the background. In this note we describe in detail a Monte Carlo event generator for the process $\bar{p}p \to \pi^+\pi^-$, when both the proton target and the antiproton beam are unpolarized. The parametrization of the input cross section is based both on data and on theoretical predictions, depending on the considered kinematic range. In those regions of the phase space not covered by the data or where the theoretical predictions are not expected to be reliable, an interpolated cross section was first obtained using the available inputs. The continuous antiproton momentum range from 0.79 GeV to 12.0 GeV in the LAB frame was fully covered in this way.

2 Kinematics

Throughout this note, the components p^μ of a generic four-momentum p are labelled by the integer index μ, which takes the values $\mu = 0, 1, 2, 3$. The temporal componet p^0 refers to the energy E and the spatial components p^i, with $i = 1, 2, 3$, to the 3-dimensional part $\mathbf{p}$ of the four-momentum. Therefore, we write $p = (E, \mathbf{p})$. The Minkowski metric with signature $g = \mathrm{diag}(+, -, -, -)$ is used. With this choice, the square of the four-momentum becomes $p^2 = p^T\, g\, p = E^2 - \mathbf{p}^2$, where the superscript T stands for matrix transpose. On-shell particles therefore satisfy the relation $p^2 = E^2 - \mathbf{p}^2 = m^2$, where m is the mass of the particle.

The kinematic description of the process $\bar{p}(p_1)\ p(p_2) \to \pi^+(p_3)\ \pi^-(p_4)$ starts by choosing a specific reference frame to which the particle four-momenta $p_1,\ p_2,\ p_3$ and p_4 are referred to.

Two frames will be found to be useful in our analysis: the *laboratory frame*, or LAB frame for short, and the $\bar{p}p$ *center of mass frame*, or CM frame for short.

The LAB frame is a coordinate system defined by choosing the positive z-axes aligned with the antiproton beam momentum direction and having the proton target at rest. It is the frame in which a fixed target experiment is done and therefore, where the detector is at rest. Unprimed four-vectors will be used when we refer to the LAB frame. A picture of the kinematics in the LAB frame is shown in Fig 1.

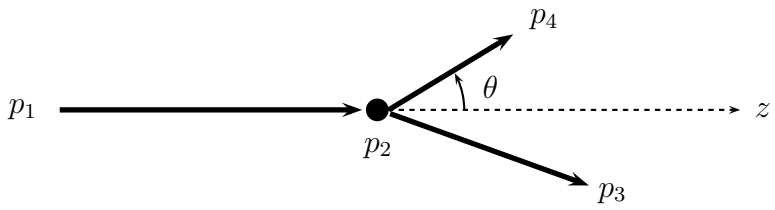

Figure 1: *Kinematics in the LAB frame.*

In the LAB frame, initial state kinematics is completely specified by a single variable. For convenience, we take this variable to be the antiproton beam momentum P. The incoming proton and antiproton four-momenta are then given by:

$$p_1 = (E, 0, 0, P) , \qquad E = \sqrt{M^2 + P^2} \tag{2.1}$$

$$p_2 = (M, 0, 0, 0) , \tag{2.2}$$

where M is the mass of the proton.

The Lorentz invariant s, defined as as the invariant mass square of the proton-antiproton system, will be a useful quantity to solve the kinematics. Using initial state LAB frame variables, it can be easily evaluated:

$$\begin{aligned} s &= (p_1 + p_2)^2 \\ &= p_1^2 + p_2^2 + 2\, p_1 \cdot p_2 \\ &= M^2 + M^2 + 2\, EM \\ &= 2\, M(M + E) . \end{aligned} \tag{2.3}$$

The CM frame is the frame where the total momentum is zero, so we have $\mathbf{p}'_1 + \mathbf{p}'_2 = 0$ Primed four-vectors will be used when we refer to the CM frame. The incoming proton and antiproton collide, therefore, head to head. Again, we choose $\mathbf{p}'_1$ to define the $+z$ direction of the coordinate system.

The parametrization of the phase space of the outgoing pions, that is, the set of all four-momenta p'_3 and p'_4 compatible with energy-momentum conservation, becomes simple in the CM frame. Momentum conservation means that we also have $\mathbf{p}'_3 + \mathbf{p}'_4 = 0$, so the outgoing pions are produced back to back in the CM frame. A picture of the kinematics in the CM frame is shown in Fig 2.

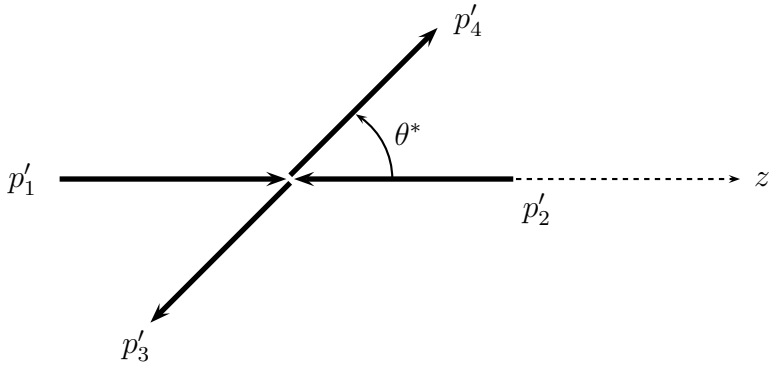

Figure 2: *Kinematics in the CM frame.*

In the CM frame, the evaluation of the Lorentz scalar s reduces to

$$s = (p'_1 + p'_2)^2 = (E'_1 + E'_2, \mathbf{p}'_1 + \mathbf{p}'_2)^2 = (E'_1 + E'_2)^2 \ , \tag{2.4}$$

and therefore s is called the *center of mass energy squared*.

Because for the two outgoing particles we have $\mathbf{p}'_3 + \mathbf{p}'_4 = 0$ and $m_3 = m_4 = m_\pi$, they are produced with the same energy, so $E'_3 = E'_4$. Energy conservation then means that each of them takes exactly half of the available energy in the CM frame:

$$E'_3 = E'_4 = \frac{\sqrt{s}}{2} \ , \tag{2.5}$$

which fixes the modulus of the momentum carried by each one of the pions:

$$|\mathbf{p}'_3| = |\mathbf{p}'_4| = \sqrt{\frac{s}{4} - m_\pi^2} \ . \tag{2.6}$$

The only degrees of freedon that are still left to completely fix the kinematics of the final state are the polar and azimuthal angles in the CM frame θ^* and ϕ^* of one of the two pions. For convenience, we choose the negative charged pion as the reference. A more natural parametrization of the phase space is yielded by taking, instead of θ^*, $\cos\theta^*$ as an independent variable. $\cos\theta^*$ can take any value in the interval $[-1, 1]$ and ϕ^* and take any

value in the interval $[0, 2\pi]$. The variables $\cos\theta^*$ and ϕ^* completely parametrize the phase space of the outgoing pions in the CM frame:

$$p'_3 = (E'_4, -\mathbf{p}'_4) \ , \qquad \mathbf{p}'_4 = |\mathbf{p}'_4|(\sin\theta^*\cos\phi^*, \sin\theta^*\sin\phi^*, \cos\theta^*) \tag{2.7}$$

$$p'_4 = (E'_4, \mathbf{p}'_4) \tag{2.8}$$

The choice of the antiproton beam momentum direction to define z-axes in both the CM and LAB frames implies that the transition from one to the other is given by a Lorentz boost Λ along the momentum third component. The Lorentz boost then mixes the energy and z-component of the a generic four-momentum k , while leaving the transverse components x and y unchanged. The explicit implementation of the non-trivial part of the boost is given by

$$\begin{pmatrix} k^0 \\ k_z \end{pmatrix} = \begin{pmatrix} \gamma & \sqrt{\gamma^2-1} \\ \sqrt{\gamma^2-1} & \gamma \end{pmatrix} \begin{pmatrix} k^{0\,\prime} \\ k'_z \end{pmatrix} \ , \qquad \gamma = \frac{\sqrt{s}}{2M} \ . \tag{2.9}$$

After boosting the two pion final state to the LAB frame, the resulting momenta p_3 and p_4 constitute the final event record:

$$\begin{aligned} p'_3 \to p_3 &= \Lambda p'_3 \\ p'_4 \to p_4 &= \Lambda p'_4 \ . \end{aligned} \tag{2.10}$$

3 The cross section

Currently, there is no single description for the cross section which is valid in the full kinematic range. For this reason, the parametrisation of the cross section was considered independently in different kinematic regions according to the data and theoretical predictions available in each case. Attending to the antiproton beam momentum in the LAB frame, three main regions are distinguished: the *low energy region*, the *transition region* and the *high energy region.*

The low energy region

In the antiproton momentum range $0.79 \leq P \leq 2.43$ GeV, data from the CERN 28 GeV proton synchrotron [4] were used to parametrise the cross section. The differential cross section per unit of solid angle $d\sigma/d\Omega$, where the solid angle element is defined in the usual way as $d\Omega = d\cos\theta^* d\phi^*$, was measured for 20 incident momenta of the antiproton beam as a function of $\cos\theta^*$, covering the angular range $|\cos\theta^*| < 0.94$ in a total of 48 bins.

Following the authors, at each momentum the data were fitted with a Legendre polynomial series:

$$\frac{d\sigma}{d\Omega} = \sum_{n=0}^{n_{\max}} a_n \, P_n(\cos\theta^*) \ , \tag{3.1}$$

where P_n is the Legendre polynomial of order n and the coeficients a_n are taken as the free parameters of the fit. At the highest momentum, several orders of fit were examined. The number of terms in the series was increased until there was no significant improvement in the χ^2 per degree of freedom, which then plateaued at a value closed to unity. For consistency, the same number of terms was then used throughout the momentum range, even though the cross section at lower momenta could be fitted adequately with fewer terms. Coeficients up to a_{10} were used. The fitted cross section are plotted at each of the incident momenta in Figs. 3, 4, 5, 6 and 7.

For reasons that will become clear later, at the highest antiproton momentum $P = 2.43$ GeV, the cross section $d\sigma/dt$, where t is the Mandelstam variable $t = -(p_1 - p_4)^2$, was calculated from the corresponding $d\sigma/d\Omega$. The mapping from $\cos\theta^*$ to t can be obtained by expanding the squared in the CM frame:

$$\begin{aligned} t &= -(p_1' - p_4')^2 \\ &= -({p_1'}^2 + {p_4'}^2 - 2p_1' \cdot p_4') \\ &= -(M^2 + m_\pi^2 - 2\,E_1' E_4' + 2|\mathbf{p_1'}||\mathbf{p_4'}|\cos\theta^*) \ , \end{aligned} \tag{3.2}$$

from which differentiation yields the relation between $\cos\theta^*$ and t-bins:

$$dt = 2|\mathbf{p_1'}||\mathbf{p_4'}| d(\cos\theta^*) \ . \tag{3.3}$$

The relation between both cross sections is then given after an integrating in the azimuthal variable ϕ^*:

$$\begin{aligned} \frac{d\sigma}{dt} &= \frac{1}{2|\mathbf{p_1'}||\mathbf{p_4'}|} \frac{d\sigma}{d(\cos\theta^*)} \\ &= \frac{1}{2|\mathbf{p_1'}||\mathbf{p_4'}|} \int_0^{2\pi} d\phi^* \frac{d\sigma}{d(\cos\theta^*) d\phi^*} \\ &= \frac{\pi}{|\mathbf{p_1'}||\mathbf{p_4'}|} \frac{d\sigma}{d\Omega} \ . \end{aligned} \tag{3.4}$$

At the highest momentum $P = 2.43$ GeV, the constant factor $\pi/|\mathbf{p_1'}||\mathbf{p_4'}|$ takes the value 2.77 GeV^{-2}. The corresponding cross section $d\sigma/dt$ as a function of $\cos\theta^*$ is plotted in Fig. 8

The high energy region

In the antiproton momentum range $5.0 \leq P \leq 12.0$ GeV, the very recent predictions by J. Van de Wiele and S. Ong were used to parametrise the cross section [5]. Their Regge-inspired phenomenological model, based on the trajectories exchanged in the t and u channels, is expected to be valid at large values of the center of mass energy squared s. The comparison between the differential cross sections predictions and the available data [6, 7, 8] is done to determine the values of the few parameters of the model. Numerical values of $d\sigma/dt$ were provided by the authors at 15 incident momenta of the antiproton beam as a function of $\cos\theta^*$ [9]. The lattice spacing in momentum was 0.5 GeV and the lattice spacing in $\cos\theta^*$ was 0.01.

The transition energy region

In the antiproton momentum range $2.43 < P < 5.0$ GeV no data were available to parametrise the cross section by an appropiate fit or to constrain the parameters of a phenomenological model. The Regge theory approach used in the high energy region was extrapolated from antiproton momentum 5.0 GeV down to 3.0 GeV, limit in which its predictions are not expected to be valid any more. In a similar way, numerical values of $d\sigma/dt$ were provided by the authors at 4 incident momenta of the antiproton beam in this range, as a function of $\cos\theta^*$ [9]. As in the previous case, lattice spacing in momentum was 0.5 GeV and the lattice spacing in $\cos\theta^*$ was 0.01. The momentum range $2.43 < P < 3.0$ GeV left a gap where no data or theoretical predictions were available.

The cross section in the full $(P, \cos\theta^*)$ space

According to the description just given, an input value for either $d\sigma/d\Omega$ or $d\sigma/dt$ (from data or from theoretical prediction) was available only at particular values of antiproton beam momentum P and $\cos\theta^*$. In those points $(P, \cos\theta^*)$ without an input cross section, linear nearest neighbor interpolation was applied to extract a value. In the momentum range $2.43 < P < 3.0$ GeV, the cross section $d\sigma/dt$ at both extremes was used cosistently to do the interpolation at momentum values in between. With this procedure, the value of the cross section is available in the antiproton momentum range $0.79 \leq P \leq 12.0$ GeV and $-1 \leq \cos\theta^* \leq 1$, where the P and $\cos\theta^*$ can take any value within the specified limits.

4 Sampling the cross section

The differential cross section $d\sigma/d\Omega$ and $d\sigma/dt$ as a function of $\cos\theta^*$ was the starting point for the event generation in the antiproton momentum range $0.79 \leq P \leq 2.43$ GeV and $2.43 < P \leq 12.0$ GeV, respectively. The event generatation proceeds with the simple "accept/reject" method. First, in the initialisation stage, an upper bound C for the cross section at the user defined antiproron momentum P, is determined. Then, in the event loop stage, the cross section is repeatedly sampled and tested as follows until the desired number of events is reached: 1) a value for $\cos\theta^*$ is generated randomly in the user defined interval $[\cos\theta^*_{min}, \cos\theta^*_{max}]$ with flat probability density, and the value is used to calculate the cross section; 2) a second random variable y is generated uniformly in the range $[0, C]$; 3) if y is larger than the value of the cross section, the event is discarded and the cross section resampled (step 1); otherwise 4) the event is accepted, a value ϕ^* is uniformly generated in the range $[0, 2\pi]$ and 5) the event is built by calculating the two pion final state four-momenta out of the generated $\cos\theta^*$ and ϕ^* according to the description given in Section 2.

The pseudo ramdom number generator used to produced uniformly distributed random numbers in the interval $[0, 1)$ was RANLUX [10], whose source code [11] was added to our program. Typical generation times were found to be of the order of 30 μ sec per accepted event.

5 Routines in the generator

A brief description of all routines used by the generator is provided here.

- `mz_pp_to_pipi_vandewi_init`: it checks if all user defined parameters have their values in the allowed ranges, otherwise it stopps the job; it determines the kinematic region corresponding to the input antiproton momentum as well as the parametrization of the cross section to be used and determines whether or not interpolation of the cross section between two momentum values is needed; it initialises the random number generator and prints out to the log file basic kinematic information.

- `mz_pp_to_pipi_get_p_lattice_site`: it determines whether or not the input antiproton momentum corresponds to one of sites of the momentum lattice. In the negative case, it determines the two sites on the momentum lattice which will be used to interpolate the cross section.

- `mz_pp_to_pipi_get_costheta_lattice_site`: In both the transition and high energy region, it determines whether or not the generated $\cos\theta^*$ corresponds to one of sites of the $\cos\theta^*$ lattice. In the negative case, it determines the two sites on the $\cos\theta^*$ lattice which will be used to interpolate the cross section.

- `mz_pp_to_pipi_vandewi_maximum_sigma`: it determines an upper bound to the cross section for the input antiproton momentum in the full $\cos\theta^*$ range.

- `mz_pp_to_pipi_vandewi_sigma_legendre`: in the low energy region, it returns the value of $d\sigma/d\Omega$ at the i-th site on the momentum lattice for the generated $\cos\theta^*$.

- `mz_pp_to_pipi_vandewi_sigma`: it returns the value of the cross section for the input antiproton momentum at the generated $\cos\theta^*$, performing all momentum and $\cos\theta^*$ interpolations whenever is necessary. If the antiproton momentum belongs to the low energy region, it returns the value $d\sigma/d\Omega$, otherwise it returns the value $d\sigma/dt$.

- `mz_pp_to_pipi_vandewi_event`: it generates one physical event by returning the four-momenta of the two charged pions in the final state, in the LAB frame.

- `mzvmod2`: it returns the square of an input four-vector.

- `mz_legendre_polynomial`: it returns the value of the n-order Legendre polynomial at any $-1 \leq x < 1$, up to order 10.

- `mz_linear_interpolation`: it interpolates a linear function $y = ax + b$ between two points (x_1, y_1) and (x_2, y_2) and returns its value at the input x.

- `mzrnd`: it returns a random number generated with flat probability density in the in the interval $[a, b]$ using RANLUX.

- `mzboost`: it boosts the four momenta of the two pions in the final state from the CM frame to the LAB frame.

6 Interface to PandaRoot

The $\bar{p}p \to \pi^+\pi^-$ event generator has been successfully interfaced to PandaRoot, so the output is directly streamed to the simulation framework during execution time, event by event. All source files can be found in `/pandaroot/pgenerators/EMFFgenerators`. The files PndPiPiGenerator.* contain the interface class, which is responsible of the communication between

the original event generator source code and PandaRoot. The class receives particle momenta from the event generator and pass this information efficiently to PandaRoot, which then procceds with the simulation stage. Sucessful compilation of the generator within the simulation framework was achieved by aplying the appropiate modifications to the CMakeLists.txt files.

7 User guide

The set of parameters needed by the generator are suplied and passed to the program in the simulation macro, where the generator is called. The user has to provide the following data:

- P: antiproton beam momentum in the lab frame, in GeV. The allowed range is $0.79 \leq P \leq 12.0$ GeV. Setting a value below the PANDA threshold $0.79 \leq P < 1.5$ GeV is possible, but a warning message will be printed out to the log file.
- *seed*: the initialisation seed fixing the state in RANLUX, an integer in the range $[1, 2^{31})$.
- $\cos\theta^*_{min}$ and $\cos\theta^*_{max}$: minimum and maximum values, respectively, of $\cos\theta^*$. The allowed range is $-1 \leq \cos\theta^*_{min} < \cos\theta^*_{max} \leq 1$. However, for antiproton momentum in the interval $0.79 < P < 2.43$ GeV (i.e. the low energy region), it is recomended to limit the angular range to $-0.94 < \cos\theta^*_{min} < \cos\theta^*_{max} < 0.94$, as in this range the cross section in the very forward or very backward region may be affected by large extrapolations resulting from extending the fits results beyond the measurements range. Exceeding these limits is possible, but warning message will be printed out to the log file.

As already mentioned, the program checks that all user defined parameters take their value in the allowed ranges, stopping the job when this condition is not satisfied. An example simulation macro is given in Appendix A

8 Examples

The generator has been examined carefully in order to check that the resulting distributions at the Monte Carlo true level agree with the expectations. Figs. 9, 10 and 11 show example distributions of $\cos\theta^*$ for generated events in the low, transition and high energy regimes, respectively. In all cases, the resulting distribution follows the corresponding cross section

$d\sigma/d\Omega$ or $d\sigma/dt$. The kinematics of the two body decay in the $\bar{p}p$ CM frame becomes manifest in Fig. 12, where the production of the two outgoing pions in a "back to back" configuration with the expected energy $\sqrt{s}/2$ and flat azymuthal distribution is clearly shown. The distribution of a few variables after boosting the events to the LAB frame is shown Fig. 13. The energy spectrum of the negative charged pion in the LAB frame mimics the distribution of $\cos\theta^*$ in the CM frame, as corresponds to the linear mapping between these two variables induced by the boost along the momentum third component. The azimuthal flat distribution is preserved by the boost, as expected, whereas the whole sample is boosted in the forward direction, as the $\cos\theta$ distribution shows.

9 Summary

A Monte Carlo event generator which simulates the $\pi^+\pi^-$ production in $\bar{p}p$ annihilations, when both the proton target and the antiproton beam are unpolarized, has been described. The cross section used for the event generation was parametrised in terms of a Legendre polynomial series fitted to data from the CERN 28 GeV proton synchroton in the low energy regime, whereas in the high energy regime the recent theoretical predictions by J. van de Wiele and S. Ong were used. An interpolated cross section was extracted in those $(P, \cos\theta^*)$ points not covered by the measurements or by the available theoretical predictions. The antiproton momentum range in the LAB frame extends from 0.79 GeV to 12.0 GeV. For each momentum, the full range $-1 \leq \cos\theta \leq 1$ was covered. The generator can be used as a useful tool to study pion production at PANDA, both for the development of efficient algorithms for pion rejection and for the measurement of $\pi^+\pi^-$ production cross section in proton-antiproton annihilations.

Acknowledgements

This work has been supported by BMBF/FAIR-Panda and Helmholtz Institute Mainz. We are indebted to J. Van de Wiele and S. Ong for providing us with their cross section predictions, as well as many useful discussions and lots of explanations. We are very grateful to Stefano Spataro and the PANDA Computing Group for their help and support with the technicalities of PandaRoot. We would like to thank the KPH-Mainz PANDA group for constant encouragement and constructive remarks, in particular Frank Maas and Cristina

Morales for a careful reading of the manuscript.

A An example simulation macro

For the convenience of the user, we provide in this appendix the example simulation macro `Simulation_Example.C` which calls the pion generator. The reader is assumed to have some familiarity in doing simulations with PANDA ROOT, so only the relevant parts related to the monte carlo generator are explicitly shown. The parameters needed by the generator, described in Section 7, are passed through the arguments of the function `Simulation_Example` in the macro.

```
Simulation_Example( Double_t P=5.0,
                    Int_t seed=1,
                    Double_t cos_theta_min = -0.8,
                    Double_t cos_theta_max = 0.8 ){


   /**
   *    PARAMETERS:
   *
   *      P:               pbar momentum LAB frame [GeV]
   *      seed:            RANLUX seed
   *      cos_theta_min:   minimum cos(theta*)
   *      cos_theta_max:   maximum cos(theta*)
   *
   *    Ranges:
   *
   *      0.79 <= P <= 12.0 GeV
   *      1 <= seed < 2^31
   *      -1 <= cos_theta_min < cos_theta_max <= 1
   */
```

...

```
    // Create and Set Event Generator
    //-------------------------------
    FairPrimaryGenerator* primGen = new FairPrimaryGenerator();
    fRun->SetGenerator(primGen);

    PndPiPiGenerator* boxGen = new PndPiPiGenerator();
    boxGen->SetBeamMom(P);
    boxGen->SetSeed(seed);
    boxGen->SetCosThetaMin(cos_theta_min);
    boxGen->SetCosThetaMax(cos_theta_max);
    primGen->AddGenerator(boxGen);

                                    ...

    exit(0);
}
```

References

[1] M. F. M. Lutz *et al.* [PANDA Collaboration], *"Physics Performance Report for PANDA: Strong Interaction Studies with Antiprotons"*, [arXiv:0903.3905 [hep-ex]].

[2] E. Tomasi-Gustafsson, M. P. Rekalo, *"New possibility for further measurements of nucleon form factors at large momentum transfer in time-like region:* $\bar{p}p \to ll,\ l = e\ or\ \mu$*"*, [arXiv:0810.4245 [hep-ph]].

[3] M. Sudol *et al.*, Eur. Phys. J. A **44**, 373-384 (2010)

[4] E. Eisenhandler *et al.*, Nuclear Physics B **96**, 109 (1975).

[5] J. Van de Wiele and S. Ong, Eur. Phys. J. A **46** (2010) 291.

[6] A. Eide *et al.*, Nucl. Phys. B **60**, 173 (1973).

[7] T. Buran *et al.*, Nucl. Phys. B **116**, 51 (1976).

[8] C. White *et al.*, Phys. Rev. D **49**, 58 (1994).

[9] J. Van de Wiele, S. Ong and M. Zambrana, private communication (unpublished), (2010).

[10] M. Lüscher, Comp. Phys. Comm. **79** (1994) 100.

[11] available online at the author web page:
`http://luscher.web.cern.ch/luscher/ranlux/index.html`.

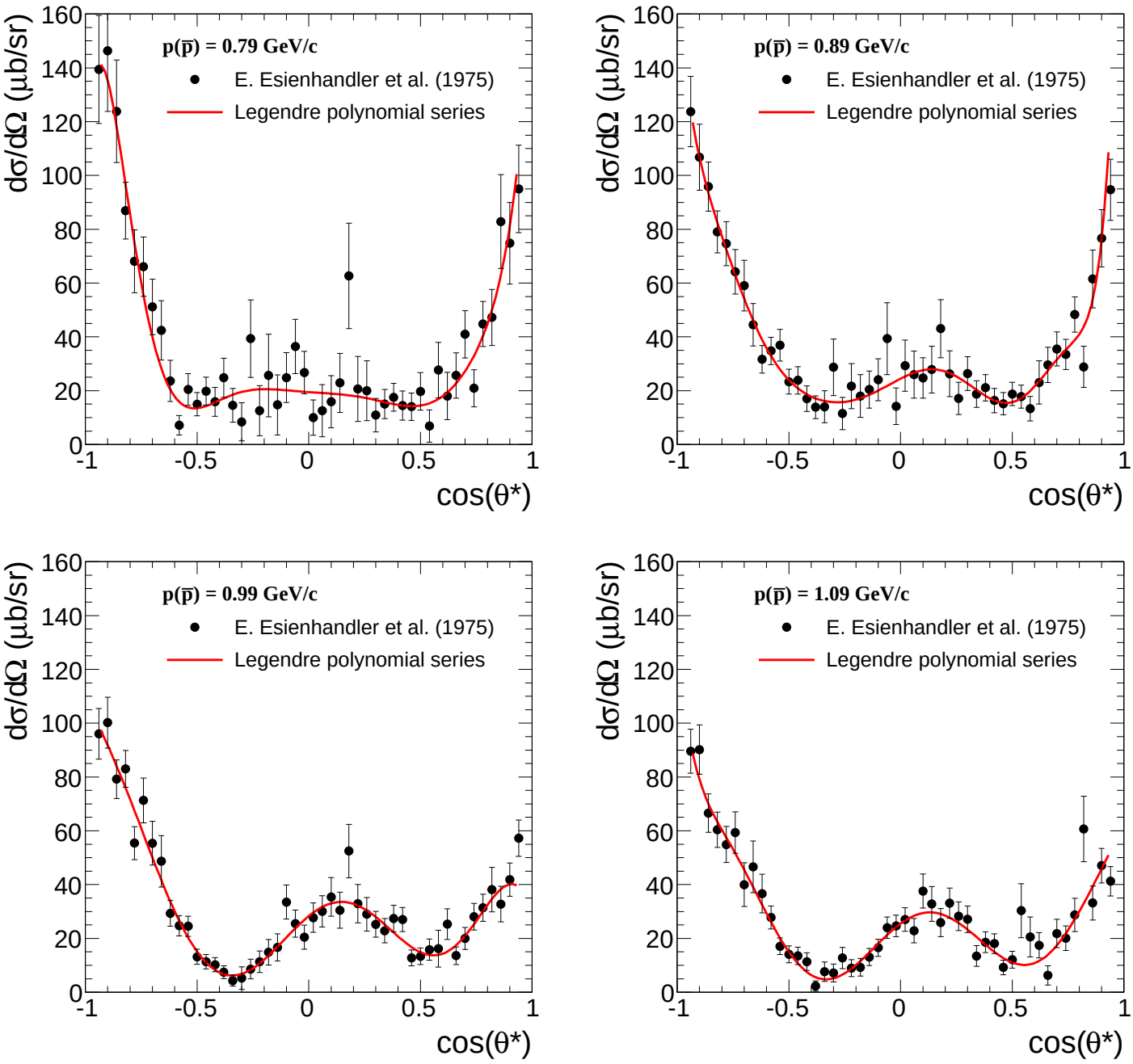

Figure 3: *Differential cross section per unit of solid angle as a function of* $\cos\theta^*$ *in the* $\bar{p}p$ *center of mass frame, for* $\bar{p}$ *momentum in the lab frame from* $0.79\ GeV$ *to* $1.09\ GeV$*. In each* $\cos\theta^*$ *bin, the plotted value is the integrated cross section in the bin divided by the bin width and by the factor* 2π*.*

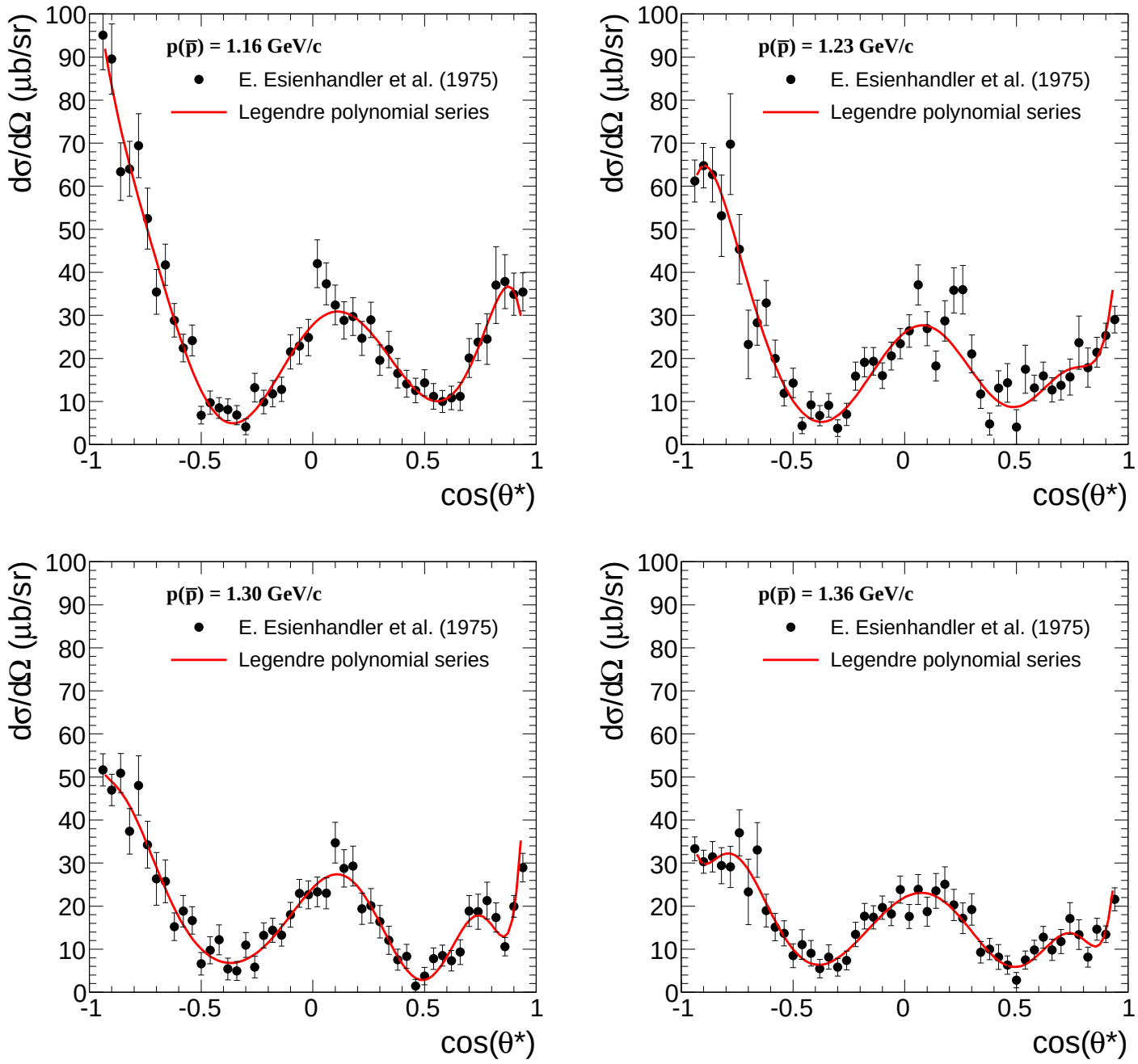

Figure 4: *Differential cross section per unit of solid angle as a function of* $\cos\theta^*$ *in the* $\bar{p}p$ *center of mass frame, for* $\bar{p}$ *momentum in the lab frame from* 1.16 *GeV to* 1.36 *GeV. In each* $\cos\theta^*$ *bin, the plotted value is the integrated cross section in the bin divided by the bin width and by the factor* 2π.

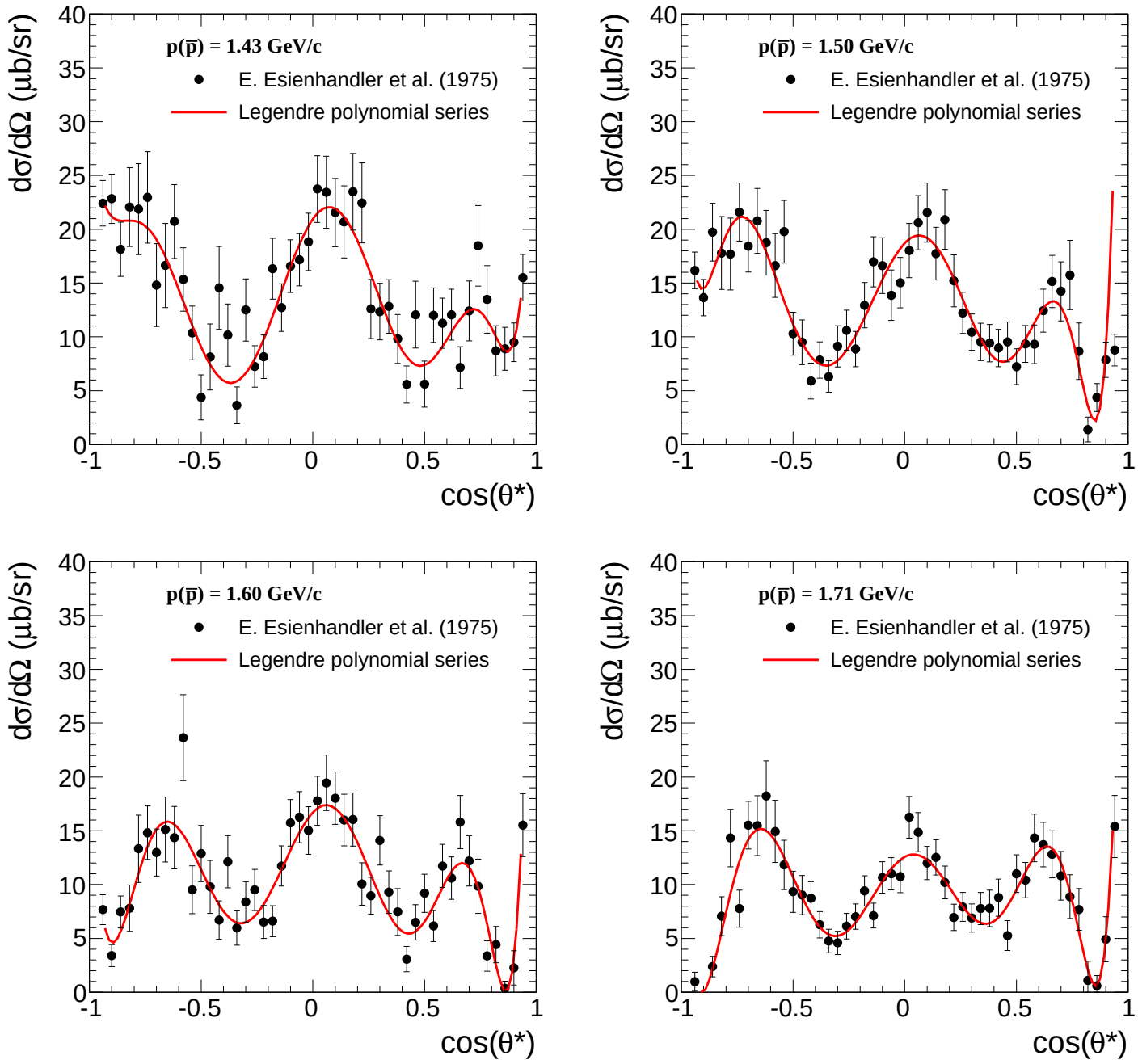

Figure 5: *Differential cross section per unit of solid angle as a function of* $\cos\theta^*$ *in the* $\bar{p}p$ *center of mass frame, for* $\bar{p}$ *momentum in the lab frame from* 1.43 *GeV to* 1.71 *GeV. In each* $\cos\theta^*$ *bin, the plotted value is the integrated cross section in the bin divided by the bin width and by the factor* 2π.

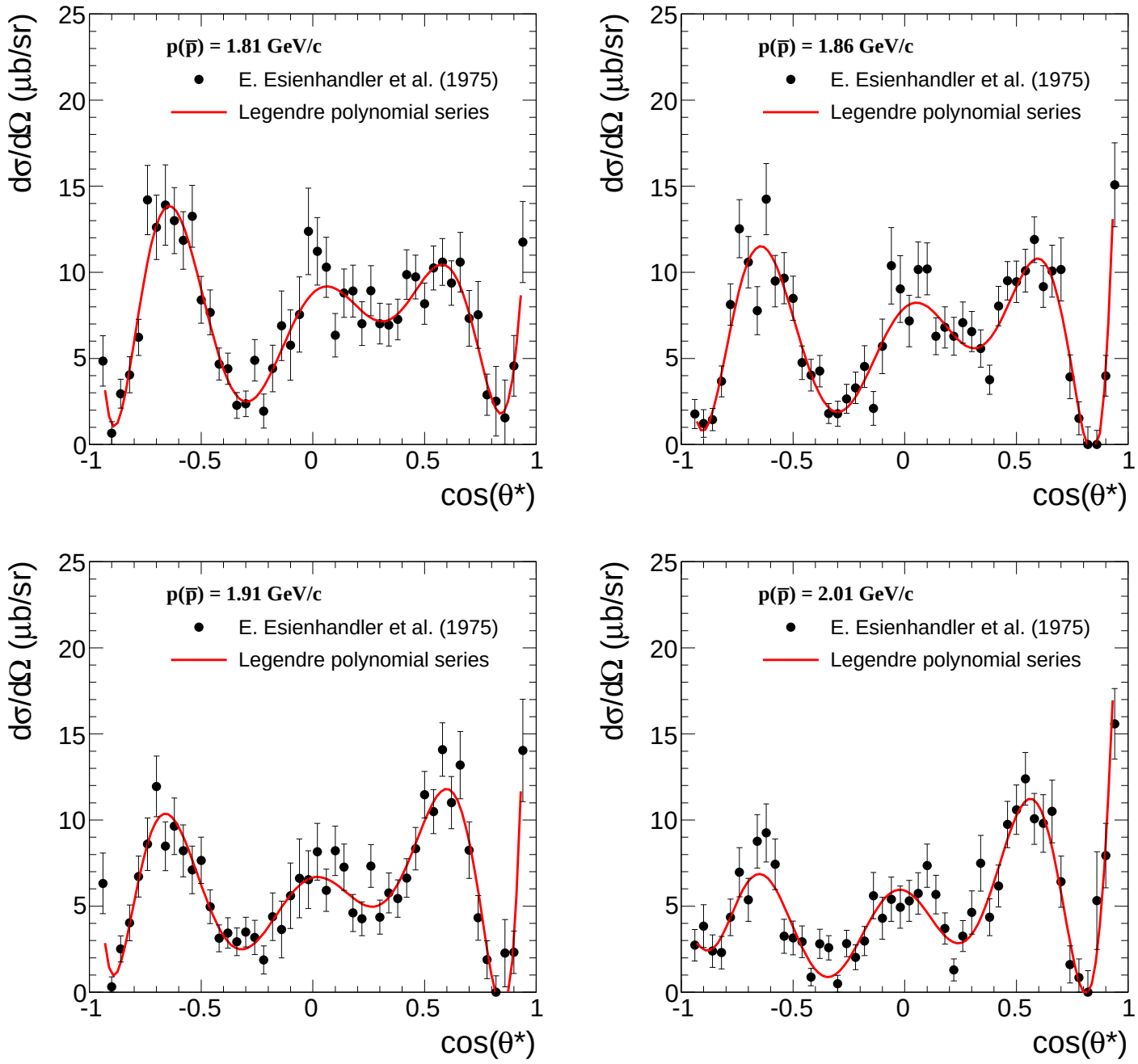

Figure 6: *Differential cross section per unit of solid angle as a function of* $\cos\theta^*$ *in the* $\bar{p}p$ *center of mass frame, for* $\bar{p}$ *momentum in the lab frame from* 1.81 *GeV to* 2.01 *GeV. In each* $\cos\theta^*$ *bin, the plotted value is the integrated cross section in the bin divided by the bin width and by the factor* 2π.

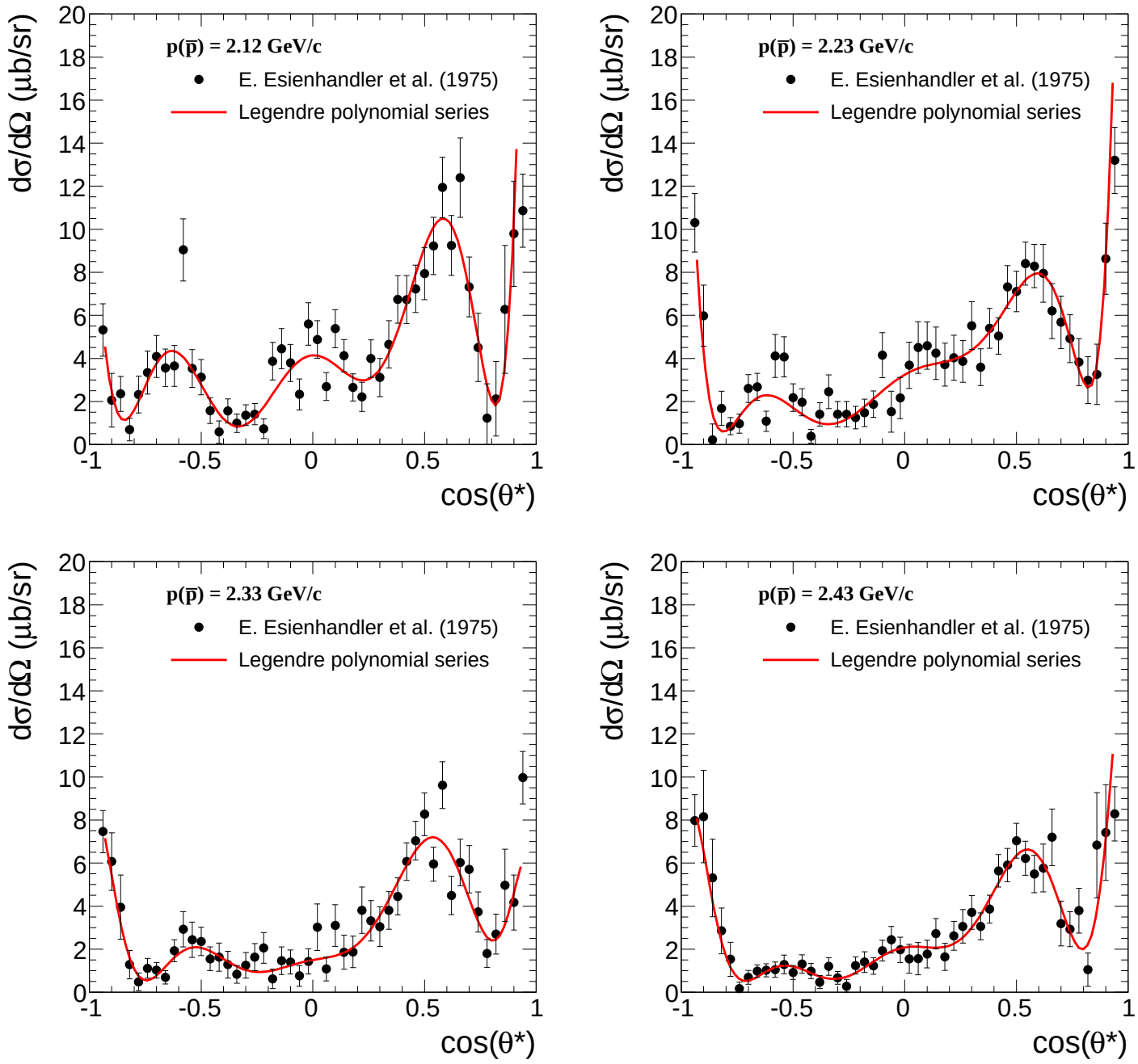

Figure 7: *Differential cross section per unit of solid angle as a function of* $\cos\theta^*$ *in the* $\bar{p}p$ *center of mass frame, for* $\bar{p}$ *momentum in the lab frame from* 2.12 *GeV to* 2.43 *GeV. In each* $\cos\theta^*$ *bin, the plotted value is the integrated cross section in the bin divided by the bin width and by the factor* 2π.

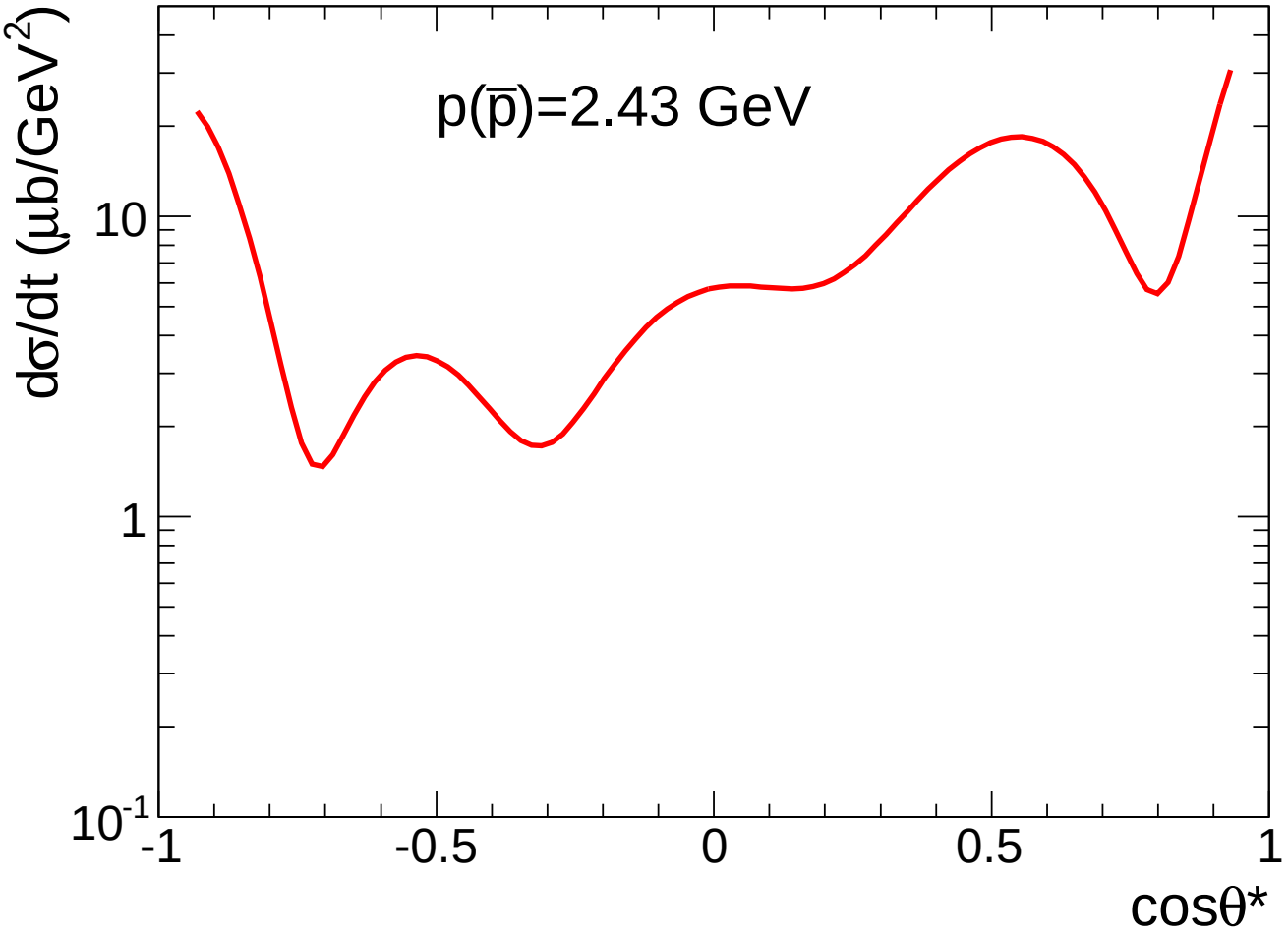

Figure 8: *Differential cross section per unit of the Mandelstam variable t as a function of* $\cos\theta^*$ *in the* $\bar{p}p$ *center of mass frame, for* $\bar{p}$ *momentum in the lab frame* 2.43 *GeV.*

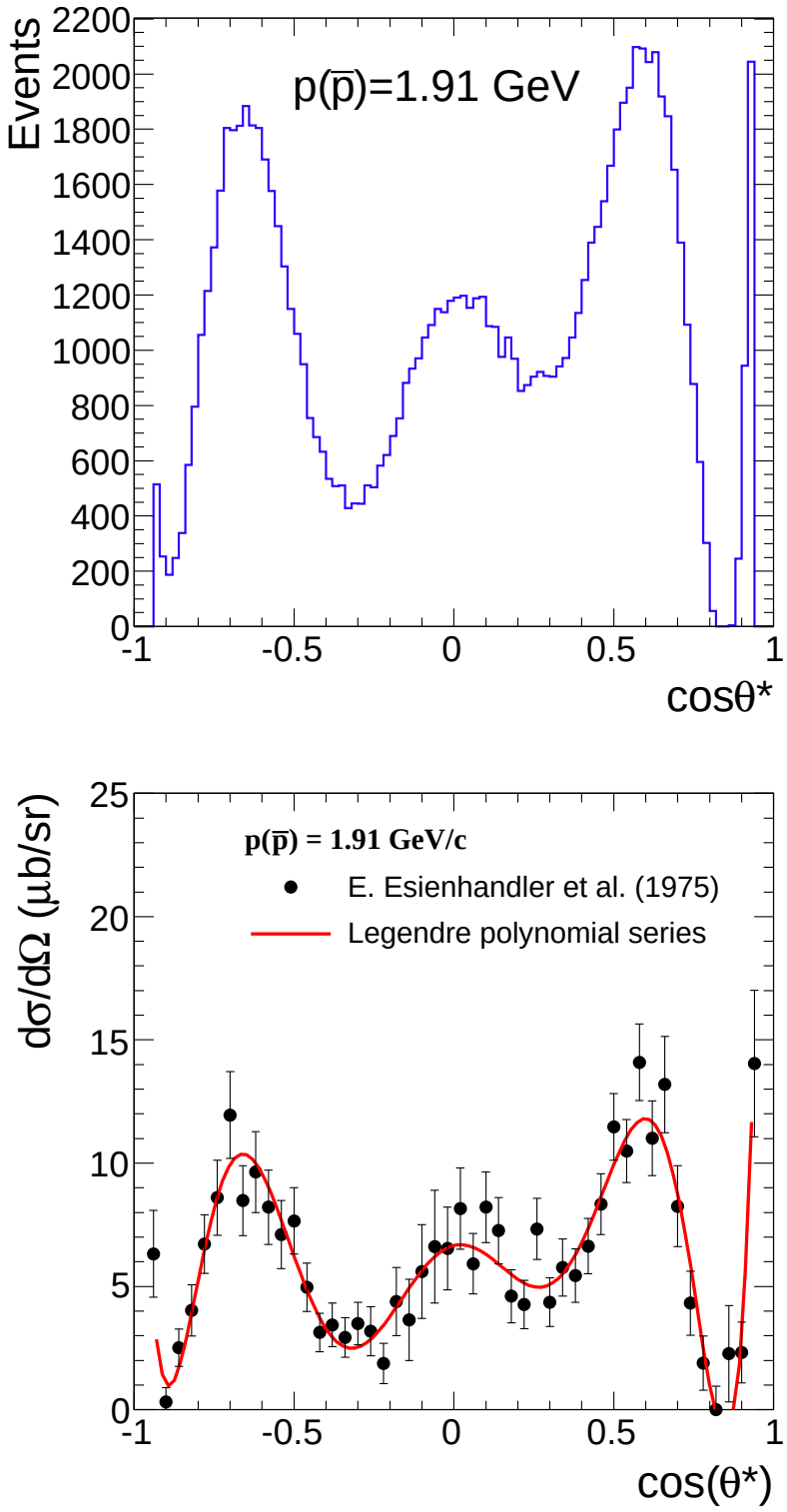

Figure 9: *Distribution of* $\cos\theta^*$ *in a sample of* 10^5 *generated events for* $\bar{p}$ *momentum in the lab frame* 1.91 *GeV in the range* $-94 < \cos\theta^* < 0.94$ *(top), in comparison to the cross section* $d\sigma/d\Omega$ *for the same momentum as a function of* $\cos\theta^*$ *(down).*

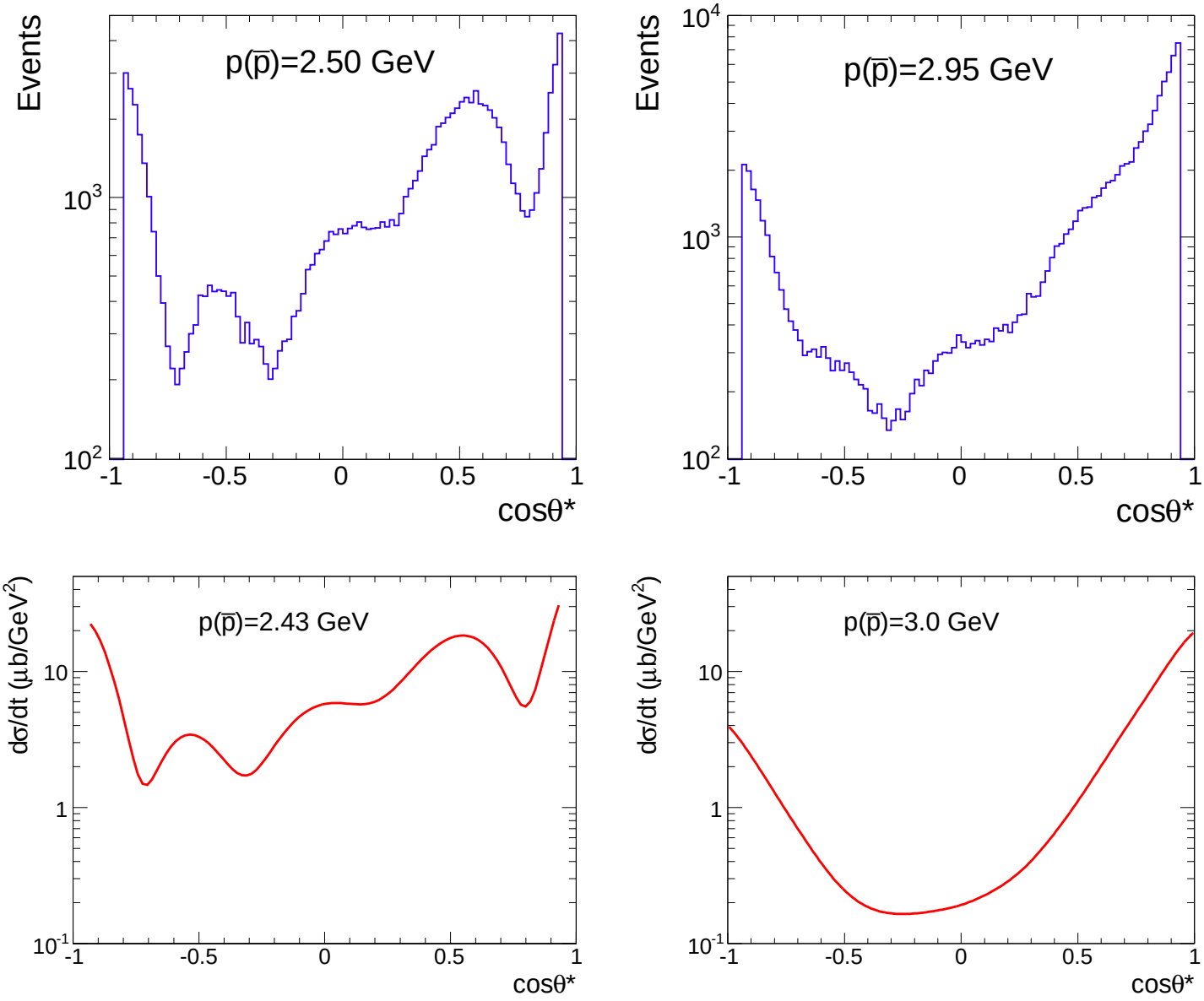

Figure 10: *Distribution of* $\cos\theta^*$ *in a sample of* 10^5 *generated events for* $\bar{p}$ *momentum in the lab frame* 2.50 *GeV and* 2.95 *GeV in the range* $-94 < \cos\theta^* < 0.94$ *(top), in comparison to the cross section* $d\sigma/dt$ *for* $\bar{p}$ *momentum* 2.43 *GeV and* 3.0 *GeV used for the interpolation as a function of* $\cos\theta^*$ *(down).*

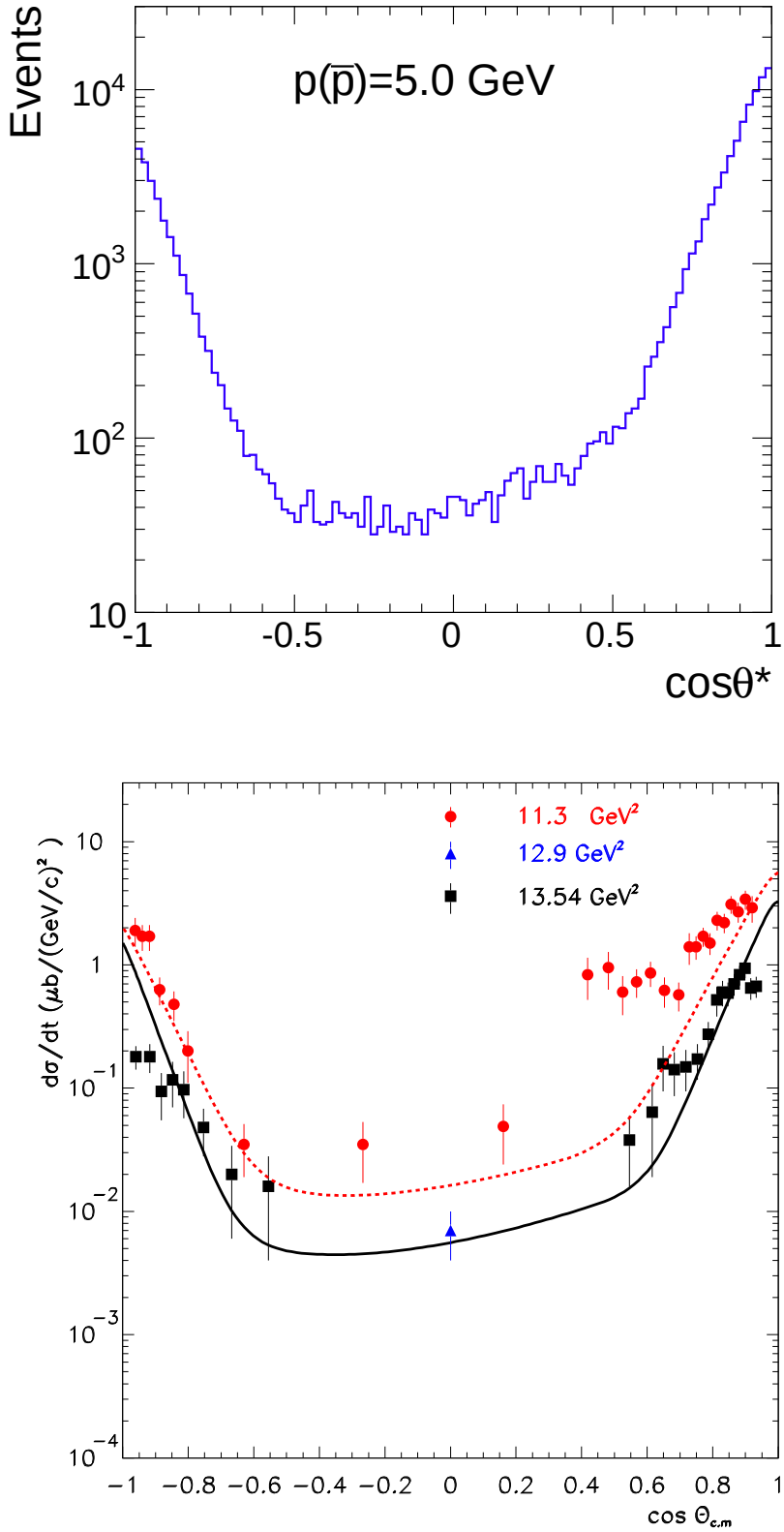

Figure 11: *Distribution of* $\cos\theta^*$ *in a sample of* 10^5 *generated events for* $\bar{p}$ *momentum in the lab frame* 5.0 *GeV (or center of mass energy square* $s = 11.3$ *GeV*^{2}*) in the range* $-1 < \cos\theta^* < 1$ *(top), in comparison to the cross section* $d\sigma/dt$ *for the same momentum as a function of* $\cos\theta^*$ *[5] (down).*

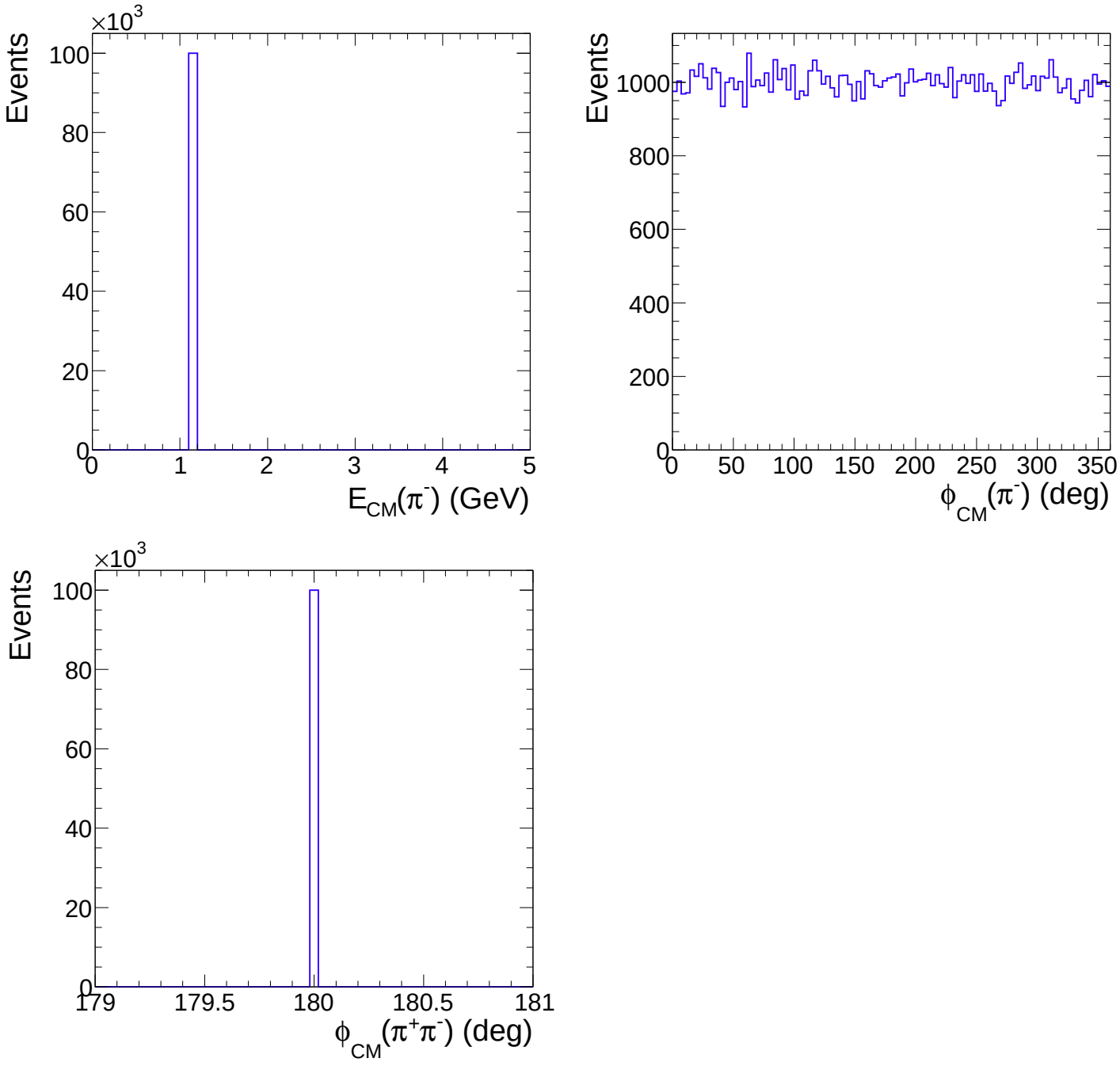

Figure 12: *The distribution of the energy and the azymuthal angle of the negative charged pions (top) and the angle between the positive and the negative charged pion (down) in the $\bar{p}p$ CM frame, in a sample of 10^5 generated events for $\bar{p}$ momentum 1.91 GeV.*

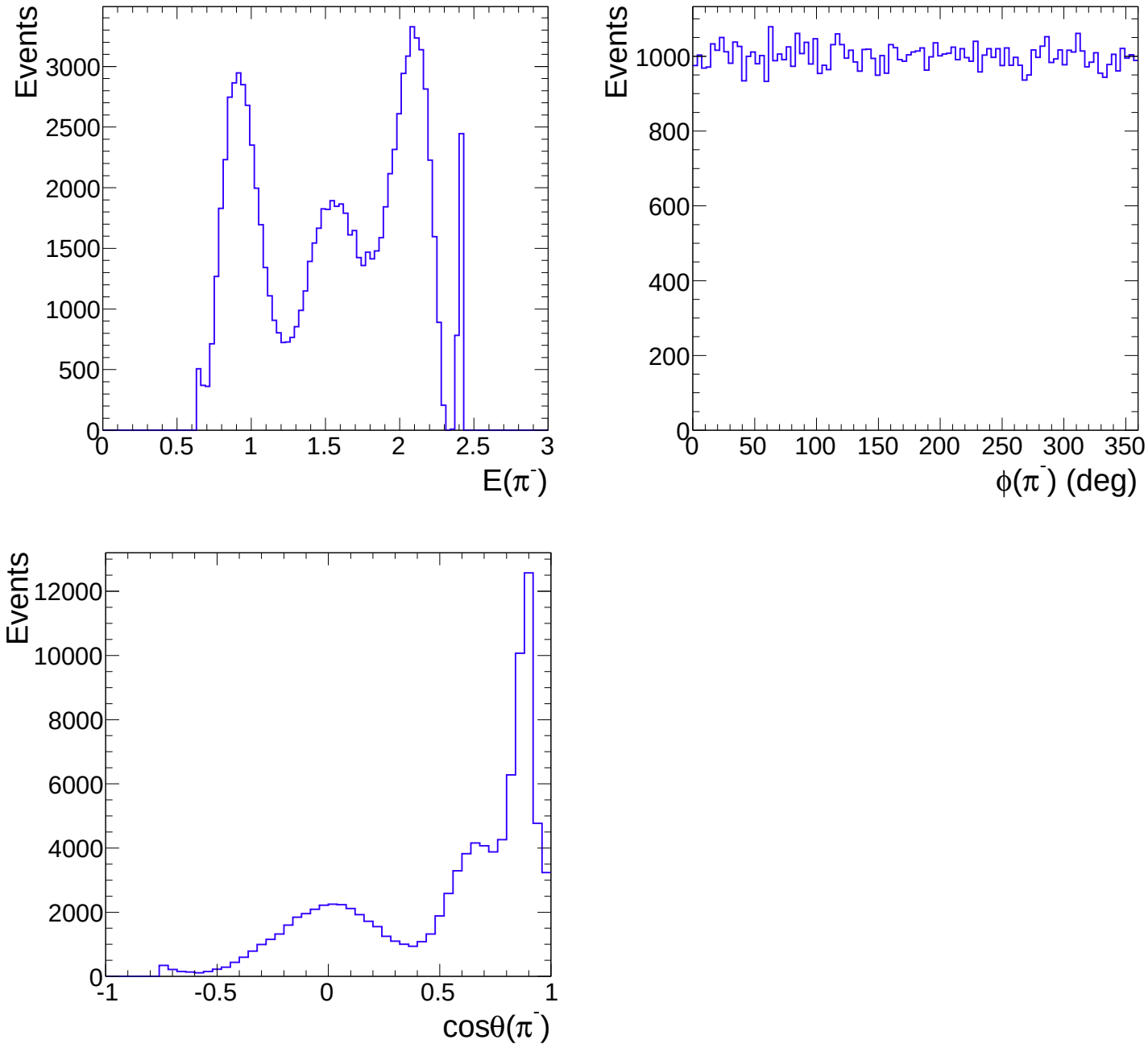

Figure 13: *The distribution of the energy and the azymuthal angle (top) and* $\cos\theta$ *(down) of the negative charged pion in the LAB frame, in a sample of* 10^5 *generated events for* $\bar{p}$ *momentum* 1.91 *GeV.*